Pluronic F127-based micelles for tumor-targeted bufalin delivery

Haijun Wang, Gareth R. Williams, Jianrong Wu, Junzi Wu, Shiwei Niu, Xiaotian Xie, Shude Li, Li-Min Zhu

PII: S0378-5173(19)30090-0
DOI: https://doi.org/10.1016/j.ijpharm.2019.01.049
Reference: IJP 18111

To appear in: *International Journal of Pharmaceutics*

Received Date: 23 October 2018
Revised Date: 17 December 2018
Accepted Date: 19 January 2019

Please cite this article as: H. Wang, G.R. Williams, J. Wu, J. Wu, S. Niu, X. Xie, S. Li, L-M. Zhu, Pluronic F127-based micelles for tumor-targeted bufalin delivery, *International Journal of Pharmaceutics* (2019), doi: https://doi.org/10.1016/j.ijpharm.2019.01.049

Pluronic F127-based micelles for tumor-targeted bufalin delivery

Haijun Wang[a], Gareth R. Williams[b], Jianrong Wu[a], Junzi Wu[a], Shiwei Niu[a], Xiaotian Xie[a], Shude Li[c,*], Li-Min Zhu[a,*]

[a] College of Chemistry, Chemical Engineering and Biotechnology, Donghua University, Shanghai, 201620, China

[b] UCL School of Pharmacy, University College London, 29-39 Brunswick Square, London, WC1N 1AX, UK

[c] Department of Biochemistry, College of Basic Medicine, Kunming Medical University, Kunming, Yunnan, 650500, China

* Corresponding authors:

E-mail address, lzhu@dhu.edu.cn (Li-Min Zhu), shudeli006@vip.sina.com (Shude Li)

ABSTRACT

In this study, we developed novel thermal and redox-responsive micelles based on the Pluronic F127 tri-block copolymer and employed these for redox-responsive intratumor release of bufalin, an anti-cancer drug. Pluronic F127 was first functionalized with carboxylate groups, and then assembled into micelles. The HOOC-F127-COOH micelles are 20 ± 4 nm in size at 37 ºC, but expand to 281 ± 5 nm when cooled to 4 ºC. This allows for the free diffusion of bufalin into the micellar cores at low temperatures, while at 37 ºC the micelles are much more compact and the drug molecules can be effectively held in their interiors. A high encapsulation efficiency and loading content were obtained via drug incorporation at 4 ºC. The drug-loaded micelles were cross-linked with cystamine, which contains a disulfide bond responsive to the local cancer microenvironment. *In vitro* studies showed that drug release from the cross-linked micelles was low under normal physiological conditions, but markedly accelerated upon exposure to conditions representative of the intracellular tumor environment. Confocal microscopy revealed that the cross-linked micelles gave high levels of drug release inside the cells. *In vivo* studies in mice showed the drug-loaded cross-linked micelles have potent anti-tumor activities, leading to high levels of apoptosis of tumor cells and significant reductions in tumor volume. The drug-loaded cross-linked micelles did not significantly influence body weight, and there was no evidence for detrimental off-target effects. These results indicate that the Pluronic-based micelles developed in this work are promising drug delivery systems for the targeted treatment of cancer.

***Keywords**:* Thermo-responsive; redox-responsive; bufalin; F127-based micelles; cross-linking; controlled release.

1. Introduction

Bufalin is a cardioactive C-24 steroid with a characteristic α-pyrone ring at C-17. It comprises the major constituent of cinobufacini injection, a traditional Chinese medicine approved by the Chinese State Food and Drug Administration (SFDA ISO9002). Cinobufacini has been used as an anti-tumor medicine for many years in China (Chen et al., 2016; Hu et al., 2014; Meng et al., 2009). Bufalin has been proven to exhibit strong antineoplastic activities, including inhibition of cell proliferation, induction of cell differentiation, induction of apoptosis, disruption of the cell cycle, inhibition of cancer angiogenesis, reversal of multi-drug resistance, and regulation of the immune response through the inhibition of Na^+, K^+-ATPase (Takai et al., 2008; Wang et al., 2014). Bufalin is involved in complex cell-signal transduction pathways and results in selective control of cancerous but not normal cellular proliferation (Newman et al., 2008; Yu et al., 2008). It is also a potent small molecule inhibitor of the steroid receptor coactivators SRC-3 and SRC-1 (which can promote SRC-3 protein degradation), and has the ability to block cancer cell growth at nanomolar concentrations (Wang et al., 2014). However, due to its insolubility in water, rapid metabolism, and short *in vivo* half-life, its application in cancer therapy is limited.

As a result of similar challenges applying to a wide range of active ingredients, there has been much interest in the development of nanoscale drug delivery systems (DDSs) in recent decades. Such systems include inorganic nanoparticles (Fan et al., 2017), liposomes (Jensen et al., 2018; Jin et al., 2018; Northfelt et al., 2013), hydrogels (Li et al., 2015; Roointan et al., 2018), polymer micelles (Fang et al., 2017; Liang et al., 2016; Wu et al., 2016) and two-dimensional materials (Lin et al., 2016; Yang et al., 2013). Polymer micelles have attracted extensive attention for cancer therapy because of their high efficiency in drug delivery and hydrodynamic stability (Gothwal et al., 2016). The amphiphilic

nature of micelles endows them with an inner hydrophobic domain, where insoluble anticancer drugs can be housed in order to increase their solubility. Their hydrophilic exterior renders micelles miscible with water, producing stable colloidal systems, and thus micellar entrapment of a drug can improve its *in vivo* drug bioavailability (Cabral et al., 2011). Despite their benefits in solubilization, however, there remains a major unmet need to achieve on-demand release from drug-loaded micelles at their target site.

The release of drugs from DDSs can be controlled by external stimuli such as pH (Duan et al., 2013; Liang et al., 2016), light (Chien et al., 2013; Cui et al., 2015), redox (Fang et al., 2017; Zhao and Liu, 2015; Zhu et al., 2017; Zou et al., 2016) or enzymatic activity (Bode et al., 2015; Liu et al., 2015), if suitable materials are chosen for their construction. pH and redox-responsive drug nanocarriers have been particularly explored because of the existence of pH and redox potential gradients between the extra- and intracellular spaces.

Pluronics (otherwise known as poloxamers, tri-block copolymers of poly(ethylene oxide)-poly (propylene oxide)-poly(ethylene oxide) [PEO-PPO-PEO]) are approved for pharmaceutical use by the US FDA (Food and Drug Administration). One widely explored member of this family is Pluronic F127, which has PPO units of 1200 kDa and a 70% PEO content. Since it has a thermo-responsive critical micelle concentration (CMC), micelles made from Pluronic F127 can be easily assembled and disassembled based on changes in temperature: this phenomenon has been widely used for the incorporation of a wide range of hydrophobic cargos (Bohorquez et al., 1999a; Zhang et al., 2016). However, Pluronic F127 micelles will dissociate into monomers in the bloodstream, where its concentration will be below the CMC. This effect will negate any benefits of micelle formation on the circulation half-life and biodistribution of an incorporated drug, and leakage of the drug cargo will arise before it reaches the target site (Arranja et al., 2014; Sutton et al., 2007).

To fully realize the benefits of Pluronics, many attempts have been made stabilize Pluronic micelles in recent years. For instance, He *et al.* synthesized core-shell structured nanocapsules of Pluronic F127 using chitosan as a cross-linker (Rao et al., 2015; Zhang et al., 2010). Small drug molecules could be effectively retained in the nanocapsules during circulation in the blood, and then freed upon reaching the tumor site. In other work, Li *et al.* used polyethylenimine (PEI) to increase the stability of Pluronic composites (Li et al., 2011). However, the potential cytotoxicity of PEI is a concern for translational and clinical applications (Fischer et al., 2003; Tseng and Jong, 2003). Moreover, these cross-linked polymer micelles are not specifically responsive to the tumor microenvironment, and as a result the drug cargo may not be selectively freed in the tumor site.

In an attempt to overcome this problem, in this study we explore a strategy utilizing thermo-responsive Pluronic F127-based polymer micelles to encapsulate bufalin, additionally employing cystamine as a redox-responsive cross-linker for tumor-targeted drug delivery. The thermo-responsive nature of the micelles should allow the production of materials with high encapsulation efficiency and loading capacity. There are high levels (~10 mM) of glutathione (GSH) and cysteine in the cytoplasm and endosomes of cancer cells (Estrela et al., 2006; Xu et al., 2015), and hence the micelles should also provide a burst of drug release at the target site *via* GSH cleaving disulfide bonds in the cystamine cross-linkers.

As shown in Scheme 1, carboxylated HOOC-F127-COOH tri-block copolymers can self-assemble into spherical micelles at 4 ºC. At this temperature, the micelles are swollen and have high wall-permeability, allowing for diffusion of free bufalin into the core. When the temperature is raised to 37 ºC, the micelles undergo a significant contraction in size, such that the walls are no longer permeable. This means that the hydrophobic bufalin can be effectively held in the core of the micelles.

Subsequently, a cross-linking process was carried out at 37 ºC to both improve the colloidal stability and regulate the drug release kinetics. After intravenous (i.v.) injection, the bufalin-loaded cross-linked micelles are expected to accumulate in the tumor site as a result of the enhanced permeation and retention (EPR) effect, leading to rapid redox-mediated drug release.

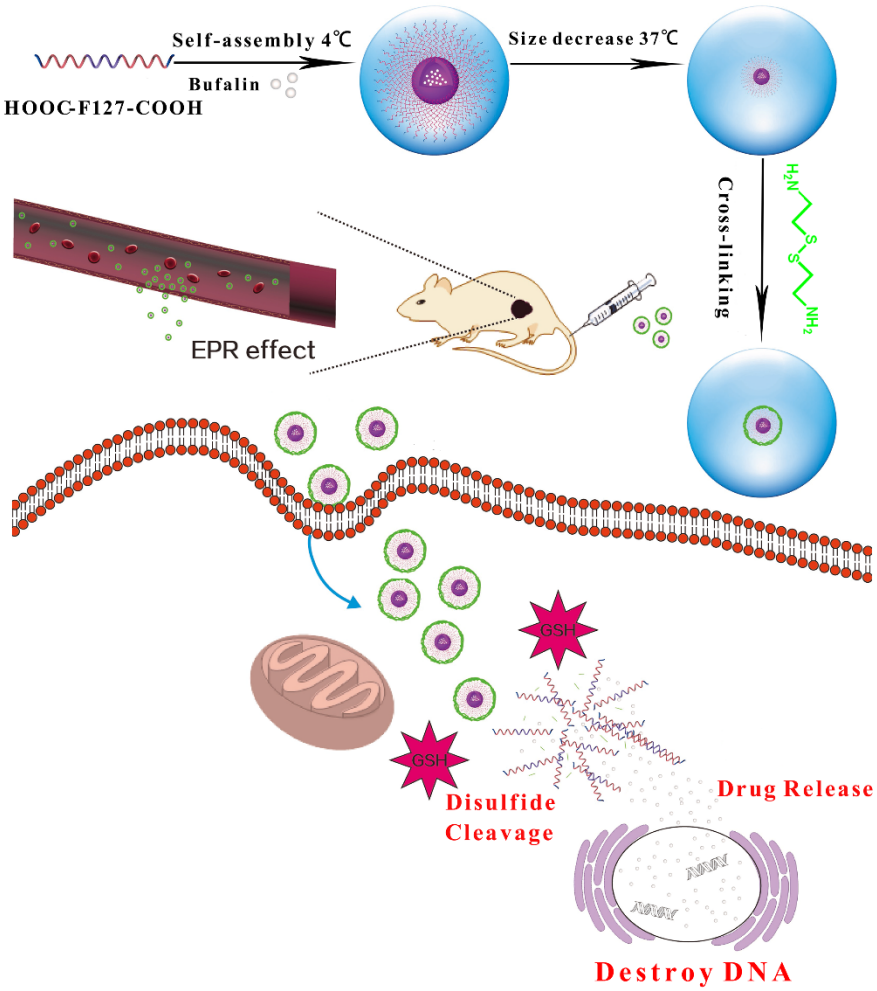

Scheme 1. The preparation of temperature and redox responsive polymer micelles, and their anti-tumor effects.

2. Materials and methods

121 *2.1. Materials*

122 Bufalin was purchased from the Baoji Herbest Bio-Tech Co., Ltd, and cystamine dihydrochloride
123 and pyrene from J&K Scientific Ltd. Pluronic F127 (MW: 12.6 kDa), maleic anhydride, toluene,
124 pyridine, N-hydroxysuccinimide (NHS), 1-(3-dimethylaminopropyl)-3-ethylcarbodiimide
125 hydrochloride (EDC·HCl), glutathione (GSH), fluorescein isothiocyanate (FITC), Hoechst 33342, and
126 3-(4,5-dimethylthiazol-2-yl)-2,5-diphenyltetrazolium bromide (MTT) were acquired from Sigma-
127 Aldrich. H22 cells (a murine hepatocellular carcinoma cell line) and L929 cells (a mouse fibroblast cell
128 line) were obtained from the Institute of Biochemistry and Cell Biology of the Chinese Academy of
129 Sciences. DMEM medium, fetal bovine serum (FBS), phosphate buffered saline (PBS), penicillin and
130 streptomycin were purchased from the Hangzhou Jinuo Biomedical Technology Co. Ltd. All other
131 chemicals were reagent grade and used as received.

132 *2.2. Synthesis of carboxylated Pluronic F127 tri-block copolymer (HOOC-F127-COOH)*

133 In order to provide carboxyl active functional groups for cross-linking, a carboxylated Pluronic
134 F127 ABA tri-block copolymer was synthesized according to the literature (Ding et al., 2011), with
135 some modifications (Scheme 2). Briefly, maleic anhydride (386 mg, 3.9 mmol) was added to a solution
136 of Pluronic F127 (5.0 g, 0.39 mmol) in a mixed solvent of toluene (20 mL) and pyridine (1 mL). The
137 reaction was carried out under stirring at room temperature for 8 h, under a nitrogen stream. The solid
138 product was filtered and precipitated in ice-cold diethyl ether three times. Next, the precipitate was
139 dried under vacuum overnight to obtain a light-brown powder comprising dicarboxylated (activated)
140 Pluronic F127. Finally, the activated Pluronic was dialyzed (MWCO 7000 Da) against deionized water
141 for 2 days to eliminate any residual maleic anhydride, toluene and pyridine. The final product was
142 obtained by lyophilization, followed by ^{1}H NMR and FTIR analysis.

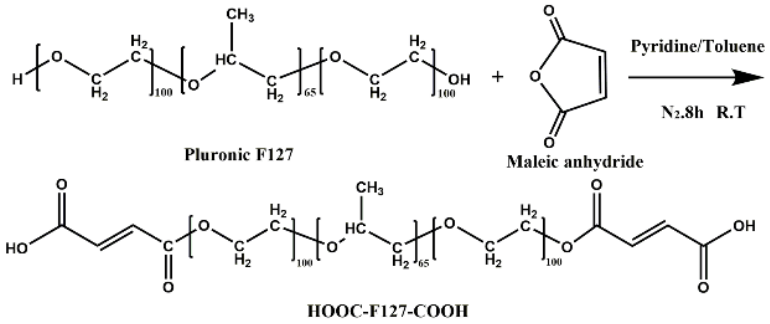

Scheme 2. The synthesis of dicarboxylated Pluronic F127 (HOOC-F127-COOH).

2.3. Preparation of bufalin loaded HOOC-F127-COOH micelles

Driven by free energy minimization, the HOOC-F127-COOH tri-block copolymer molecular chains can undergo spontaneous chain reorganization upon treatment with selected solvents, resulting in the formation of micelles. The solvophobic blocks collapse into the cores of the micelles, and the solvophilic blocks are in the coronae (Ekaterina B. Zhulina et al., 1996; Han et al., 2016). HOOC-F127-COOH micelles are similar to F127 micelles, which have a temperature-sensitive CMC (Bohorquez et al., 1999b; Rao et al., 2015). We used this thermal response to encapsulate bufalin. Briefly, a bufalin solution in methanol (20 mg in 10 mL) was mixed with HOOC-F127-COOH (200 mg). The mixture was gently stirred for 30 min, and a Labconco rotary vacuum evaporator with a water bath at 40~60 ºC then employed to evaporate the solvent. The film deposited was hydrated with 10 mL of HPLC water at 40 ºC, followed by vortexing for 10 min. The mixture was then left overnight at 4 ºC before being heated to 37 ºC and dialyzed against 1 L of deionized (DI) water at 37 ºC for 2 d, using a 7000 Da Spectra/Por dialysis tube. Finally, the sample was freeze-dried for 48 h to obtain dry bufalin loaded micelles.

2.4. Cross-linking

In order to achieve good colloidal stability, cystamine dihydrochloride was used to cross-link the micelles at 37 ºC. Bufalin loaded cross-linked micelles were prepared using a standard post-synthesis

crosslinking method (Zhao and Liu, 2015), with a small modification. Briefly, 200 mg of bufalin-loaded HOOC-F127-COOH micelles was dispersed into 50 mL of phosphate buffered saline (PBS; pH 7.4). 6.9 mg (0.06 mmol) NHS and 11.5 mg (0.06 mmol) of EDC·HCl were introduced into the above mixture. Subsequently, the suspension was stirred magnetically under a nitrogen stream overnight, in order to activate the carboxyl groups. Next, the pH value of the suspension was adjusted to 5.5 using dilute HCl, and 6.8 mg (0.03 mmol) of cystamine dihydrochloride introduced. The reaction mixture was then incubated for 24 h under nitrogen. Finally, the excess NHS, cystamine and unencapsulated bufalin were removed by dialysis for 24 h.

2.5. Analysis and characterization

^{1}H NMR spectra were recorded with a Bruker Advance 400 MHz spectrometer at room temperature, with deuterated chloroform ($CDCl_3$) as the solvent. Fourier transform infrared (FTIR) analysis was carried out on a Nicolet-Nexus 670 spectrometer over the range 4000–400 cm^{-1} and with a resolution of 1 cm^{-1}. Samples were prepared using the KBr disk method (2 mg sample in 200 mg KBr). A transmission electron microscope (TEM, JEOL 2010F) operating at 200 kV was used to characterize the morphology of the micelles and the size distribution calculated from the analysis of around 100 micelles in TEM images, using the Image J software. An aqueous solution of the sample (0.5 mg/mL) was dropped onto a carbon-coated copper grid and air dried before TEM analysis.

A pyrene fluorescent probe method was used to monitor micelle formation and determine the critical micelle concentration (CMC), following a previously reported method (Astafieva et al., 1993). 10 mL of HOOC-F127-COOH solutions at concentrations ranging from 0.05% to 2% w/v were prepared in water, with all containing the same concentration of pyrene (2.00×10^{-6} M). The solutions underwent sonication for 30 min, followed by equilibration at room temperature for 12 h in the dark.

Steady-state fluorescent spectra were measured using a QM/TM fluorescence spectrometer （PTI） with a bandwidth of 5 nm for both excitation and emission. The size of the micelles in PBS (pH 7.4) at a concentration of 2 mg/mL, with or without 10 mM GSH, was assessed at 4 ºC and 37 ºC using dynamic light scattering on a BI-200SM instrument (Brookhaven Instruments).

2.6. Drug release

The release behavior of the micelles was evaluated in triplicate in PBS (pH 7.4), using a dialysis method. Experiments were performed both with and without GSH in the release medium. The bufalin loaded micelles (20 mg) were dispersed in PBS (1.0 mL, pH 7.4), then loaded into a dialysis bag (MWCO=7000 Da) and immersed in 19 mL of PBS (pH 5.0 or 7.4) supplemented with 0/10 mM GSH. All experiments were performed at 37 ºC with shaking (100 rpm) for 48 h. At predetermined time points, 1 mL of the external medium was collected and replaced with an equal volume of fresh pre-heated medium. The concentration of the bufalin released was determined quantitatively by UV spectroscopy at 298 nm. Data are reported as mean ± standard deviation (S.D.), n=3.

2.7. Cell toxicity assays

An *in vitro* cytotoxicity investigation was performed to evaluate the biocompatibility of blank cross-linked F127-based micelles with L929 cells. In order to evaluate the antitumor and targeting ability of the drug-loaded formulations, both L929 and H22 cells were employed. L929 and H22 cells were maintained in DMEM medium supplemented with 1 % penicillin, 1 % streptomycin, and 10 % v/v fetal bovine serum. The cells were cultured as a monolayer in a humidified atmosphere containing 5 % CO_2 at 37 °C.

For cytotoxicity experiments, 200 μL of L929 or H22 cells were seeded into 96-well plates at a density of 8×10^3 cells/well. After overnight incubation at 37 ºC in a humidified 5 % CO_2 environment,

the medium was removed and fresh medium containing different concentrations of free bufalin (0.1, 0.5, 1, 5, 10, 20, 40, 60 μg/mL), or bufalin-loaded micelles (giving equivalent drug concentrations), was added to the wells. After incubation for another 24 h, 20 μL of MTT solution (5 mg/mL) was added to the wells, and the plates incubated for an additional 4 h. After this, the medium was removed, 200 μL of DMSO added to each well, and the plate thoroughly shaken for 15 min. The absorbance of the wells was finally measured at 570 nm, using a microplate reader (Multiskan FC, Thermo Scientific). The relative cell viability was calculated relative to an untreated cells control. Biocompatibility was investigated using the same protocols as described above, except that blank cross-linked F127-based micelles were added to L929 cells at final concentrations of 0.1, 1, 10, 20, 25, 50,100, 250 and 500 μg/mL. Data are reported as mean ± S.D, with three independent experiments each containing three replicates having been performed.

2.8. Cellular uptake evaluation

In order to examine the uptake and drug release of the Pluronic micelles, we first used FITC to label bufalin. Briefly, bufalin (30 mg) was dissolved in 15 mL of methanol with sonication, followed by the dropwise addition of a FITC solution in dichloromethane (10 mL, 3 mg/mL) under magnetic stirring. 50 μL of triethylamine was added to the mixture and the reaction continued for 12 h at 60 ºC in the dark, before the mixture was dialyzed against 1 L of deionized water at 4 ºC for 2 d (500 Da Spectra/Por dialysis tube). Finally, the sample was freeze-dried for 48 h to obtain dry FITC-bufalin power.

The FITC-bufalin was then encapsulated into HOOC-F127-COOH micelles, followed by cross-linking, using the same protocols as described above. For cellular uptake evaluation, 200 μL of dissociated L929 cells or H22 cells were seeded onto sterile coverslips placed in each well of a 24-well

228 culture plate (5×10^4 cells per well). 800 μL of DMEM medium supplemented with 1 % penicillin, 1
229 % streptomycin, and 10 % v/v fetal bovine serum was added to each well. After incubation for 24 h,
230 the medium was aspirated and replaced by 450 μL of fresh medium. 50 μL of a solution of free FITC-
231 bufalin or FITC-bufalin loaded micelles (each containing 20 μg/mL FITC-bufalin) was also added.
232 After incubation for 2 h (37 °C; 5% CO_2), the culture medium was removed and the cells were rinsed
233 three times with PBS. The cells were then fixed with 4 % paraformaldehyde for 20 min at 4 ºC and
234 washed with PBS three times. The cell nuclei were stained with 0.5 mL Hoechst 33342 (10 μg/mL) for
235 15 min at 37 ºC and washed with PBS three times. Finally, the cells were studied using a confocal
236 laser-scanning microscope (Carl Zeiss LSM 700) with an argon blue laser light at 488 nm and a
237 magnification of 63 ×. Each experiment was conducted in triplicate.

238 *2.9. In vivo murine tumor model*

239 24 ICR female mice (specific pathogen-free grade, 18–20 g) were procured from Jiangsu
240 KeyGEN BioTECH Co. Ltd, and all animal experiments undertaken following procedures authorized
241 by the Committee for Experimental Animal Welfare and Ethics of Kunming Medical University.
242 Tumors were induced by subcutaneous injection of 1×10^6 H22 cells in 100 μL PBS (pH = 7.2–7.4)
243 into the right front limb armpits of each mouse.

244 *2.10. In vivo antitumor efficacy*

245 The mice bearing H22 tumors were treated after the tumors reached approximately ~120 mm^3 in
246 volume. The mice were randomly divided into four groups (6 mice per group) and treated with 200 μL
247 solutions of PBS, bufalin, bufalin-loaded micelles or bufalin-loaded cross-linked micelles (giving a
248 dose of bufalin of 2 mg/kg) every two days. Tumor sizes and body weights were monitored and
249 recorded every two days for two weeks. The tumor volume was calculated as $width^2 \times length/2$.

Meanwhile, the survival rate of the mice in each group was monitored and calculated as $N_1/N_0 \times 100\%$, where N_1 and N_0 respectively denote the number of living mice and the total number of animals in each group. At the end of the monitoring period, the animals were sacrificed by cervical vertebra dislocation. The tumors and major organs of each group were extracted. The tissues were fixed with 4% paraformaldehyde solution and embedded in paraffin. The sliced organ tissues (thickness: 4 mm) were mounted on glass slides, stained by hematoxylin and eosin (H&E) and observed using a digital microscope (Nikon DS-U3) for histological analysis. The tumors tissues were further stained with terminal deoxynucleotidyl transferase dUTP nick end labeling (TUNEL) and cell apoptosis probed with a Pannoramic 250 scanning device.

3. Results and discussion

3.1. Synthesis and characterization of HOOC-F127-COOH tri-block coplolymer

In order to provide active functional groups for cross-linking, we first synthesized a carboxylated Pluronic F127 ABA triblock coplolymer. ^{1}H-NMR spectra ($CDCl_3$) showed the product to be pure, as can be seen from the spectra displayed in Figure 1. In the spectrum of as-received F127, chemical shifts (δ) can be observed at 1.2 (m), 2.2 (m), 2.6 (s), 3.4 (m), 3.5 (m); these belong to –C**H**$_3$, –C**H**–CH$_3$, –CH$_2$–O–**H**, –CH–C**H**$_2$–O–, and –O–C**H**$_2$–CH$_2$–O– group hydrogens, respectively. After functionalization we observe two new resonance peaks at δ=6.3(m) and 6.5(m) ppm, ascribed to maleic anhydride (-C**H**=C**H**-), while the δ=2.6 ppm signal coming from –CH$_2$–O**H** has disappeared. These changes in chemical shifts confirmed the introduction of carboxyl groups into F127. Successful conjugation was also confirmed by IR analysis (Supporting Information, Figure S1). The HOOC-F127-COOH material contains all the features of F127 but with additional peaks at 1730 cm^{-1} (COOH C=O stretching), and 1640 cm^{-1} (C=C stretching).

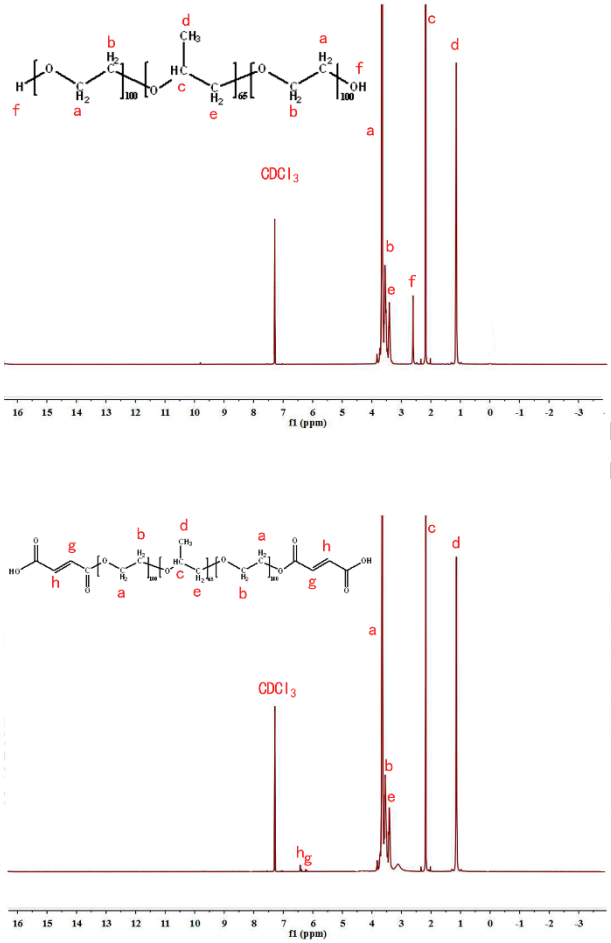

Figure 1. The ^{1}H-NMR spectra of F127 (top) and carboxylated F127 (HOOC-F127-COOH; bottom).

3.2. Micelle characterization

The I_{339}/I_{333} ratio (the ratio of the pyrene emission intensity at 372 nm with excitation at 339 nm and 333 nm) was used to determine the micellization profile and thus the critical micelle concentration (CMC) for HOOC-F127-COOH. As shown in Figure S2, the I_{339}/I_{333} changes abruptly above a concentration of 0.8 mg/mL. This represents the CMC, and is similar to the CMC stated by the supplier for F127 (0.95-1.0 mg/mL).

The size of the blank F127-based micelles was assessed *via* hydrodynamic radius measurements, with the results presented in Figure 2. The particle size of the HOOC-F127-COOH micelles was 20 ± 4

nm (PDI=0.204) at 37 ºC, and 281 ± 5 nm (PDI=0.336) at 4 ºC (Figure 2(a)). Cross-linking with cystamine caused the micelles to have a much more constant size: the crosslinked micelles have average diameter of 35 ± 4 nm (PDI=0.216) at 4 ºC and 21 ± 3 nm (PDI= 0.154) at 37 ºC (Figure 2(b)). This demonstrates that the cross-linking process was successful, and stabilized the micelles. Consequently, it is to be expected that bufalin can be effectively retained in the core of the micelles post-crosslinking. The size increase can be attributed to an increase in molecular weight after GSH inclusion, and also rearrangement of the polymer molecules in the micelles to accommodate the cross-links.

After incubation with 10 mM GSH for 4 h, the size of the cross-linked HOOC-F127-COOH micelles increased to ~293 nm (PDI=0.343) at 4 ºC and 53 nm (PDI= 0.322) at 37 ºC (Figure 2(c)). These findings indicate that GSH effectively triggers rapid disassembly of the cross-linked F127-based micelles. After GSH incubation, there is a second peak observed at ~15 nm at 4 ºC, which might be ascribed to cystamine segments cleaved from the micelles. After cleavage of the disulfide links the micelles clearly regain their thermoresponsive properties.

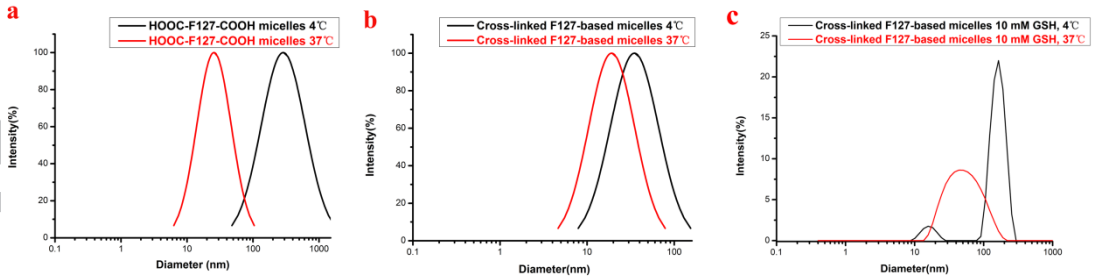

Figure 2. DLS measurements on (a) HOOC-F127-COOH micelles, (b) cross-linked F127-based micelles, and (c) cross-linked F127-based micelles following 4 h incubation with 10 mM GSH.

Typical TEM images of the blank non-cross-linked HOOC-F127-COOH micelles and bufalin

303 loaded cross-linked micelles are given in Figure 3. The micelles in both images are well dispersed and
304 appear to have roughly spherical morphologies. The diameter of the bufalin loaded cross-linked
305 micelles is a little larger than that of the non-cross-linked HOOC-F127-COOH micelles (~ 45 nm *cf.* ~
306 25 nm, respectively).

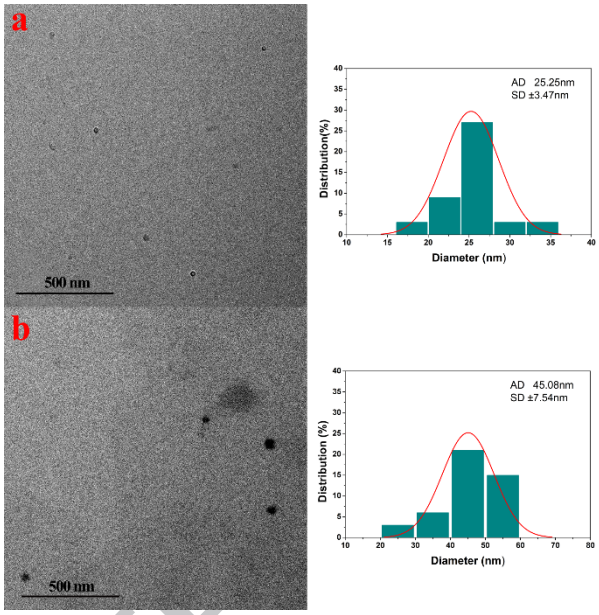

307

308 **Figure 3.** TEM images and particle size distributions of (a) non-cross-linked HOOC-F127-COOH
309 micelles, and (b) bufalin loaded cross-linked F127-based micelles.

310 *3.3 Drug loading and release behavior*

311 The bufalin encapsulation efficiency (EE %) and loading content (LC %) were determined using
312 the following equations:

313 $$\mathrm{EE\%} = \frac{\text{amount of drug in micelles}}{\text{total amount of drug in feed}} \times 100\%$$

314 $$\mathrm{LC\%} = \frac{\text{amount of drug in micelles}}{\text{total amount of drug loaded micelles}} \times 100\%$$

315 The EE and LC are 21.5 ± 1.3 % and 1.9 ± 0.2 % when bufalin is loaded into the micelles at 37 ºC, far
316 below the values obtained at 4 ºC (EE = 79.6 ± 1.2 %; LC = 2.9 ± 0.2 %).

317 The GSH level in normal tissues and blood is approximately 10 μM. In comparison, the

endosomes and lysosomes of tumor cells have high GSH levels (10 mM). The presence of cystamine as the cross-linking agent in the micelles should thus allow them to target drug release to tumor sites: the high levels of GSH there can cleave the cystamine disulfide bonds, rupturing the micelles and leading to drug release. *In vitro* release from the micelles was thus explored at 37 °C under two different conditions, in blank PBS (pH 7.4) and PBS supplemented with 10 mM GSH (Figure 4). Bufalin was released slowly from the cross-linked micelles in blank PBS, and only *ca.* 33 ± 1 % of the total drug content was released after 48 h. However, in reductive conditions (10 mM GSH, pH 7.4), bufalin was released very quickly in the early stages of the experiment. The release rate gradually declined after 12 h, and approximately 69 ± 1 % of the total incorporated bufalin was released after 48 h. The release profile of non-cross-linked micelles in blank PBS was intermediate to these (cumulative release = 51 ± 1 % after 48 h). Further, no sensitivity to GSH was observed with the non-cross-linked micelles, with the release profiles with and without the presence of GSH being superimposable. These data confirm that the F127-based micelles were successfully cross-linked, and could provide redox responsive drug release.

It is well known that the pH of the tumor environment is comparatively more acidic than physiological pH; further, and the cellular uptake of micelles most likely occurs via endocytosis or pinocytosis, which both involve lysosomal (pH 4-5) processing. Therefore, bufalin release from the cross-linked micelles at pH 5.0 was also examined (Figure 4). The release of bufalin was much faster in the simulated acidic tumor environment (PBS, pH 5.0, 10 mM GSH) than at pH 7.4, with approximately 80% release within 48 h. This is likely to be because the micelles disassemble more rapidly under acidic conditions, freeing their drug cargo as they do so (Wang et al., 2011; Yanzuo et al., 2015).

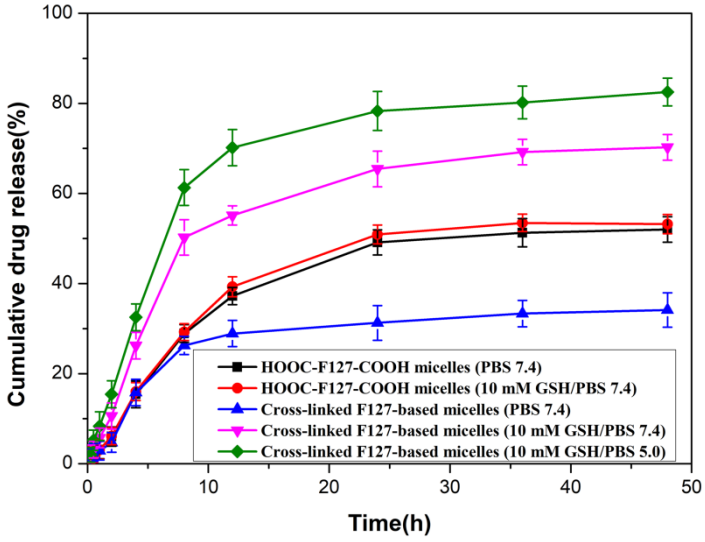

Figure 4. The release profiles of bufalin from F127-based micelles under different conditions. Data are shown as mean ± S.D. from three independent experiments.

3.4. MTT assays

The biocompatibility of the blank cross-linked micelles with healthy L929 cells was investigated using the MTT assay. As shown in Figure 5(a), no obvious toxicity was observed for the micelles even when the concentration reached 500 μg/mL. The free bufalin or drug-loaded micelles also show low toxicity to L929 cells (Figure 5(b)), with viability above 80 % even at drug concentrations of 60 μg/mL. In contrast, the bufalin loaded micelles have clear toxicity to H22 tumor cells (Figure 5(c)). As the drug concentration is raised to 60 μg/mL, the cell viability declines to 49, 40 and 28 % with free drug, drug-loaded micelles and cross-linked micelles, respectively. The drug-loaded cross-linked micelles are thus very effective at inhibiting the growth of H22 cells, but have much less influence on L929 cells. This bodes well for the development of targeted therapies. When the bufalin concentration reached 20 μg/mL and higher, it appears that the cross-linked micelles are considerably more toxic to L929 cells than the non-cross-linked micelles, however (Figure 5(b)). The reasons for this are not certain, but it may be that the smaller cross-linked micelles are more effectively endocytosed by L929 cells. The

viability of the L929 cells remains high (> 80%) even under these high concentrations of drug, presumably because of the lack of GSH in the cytosol.

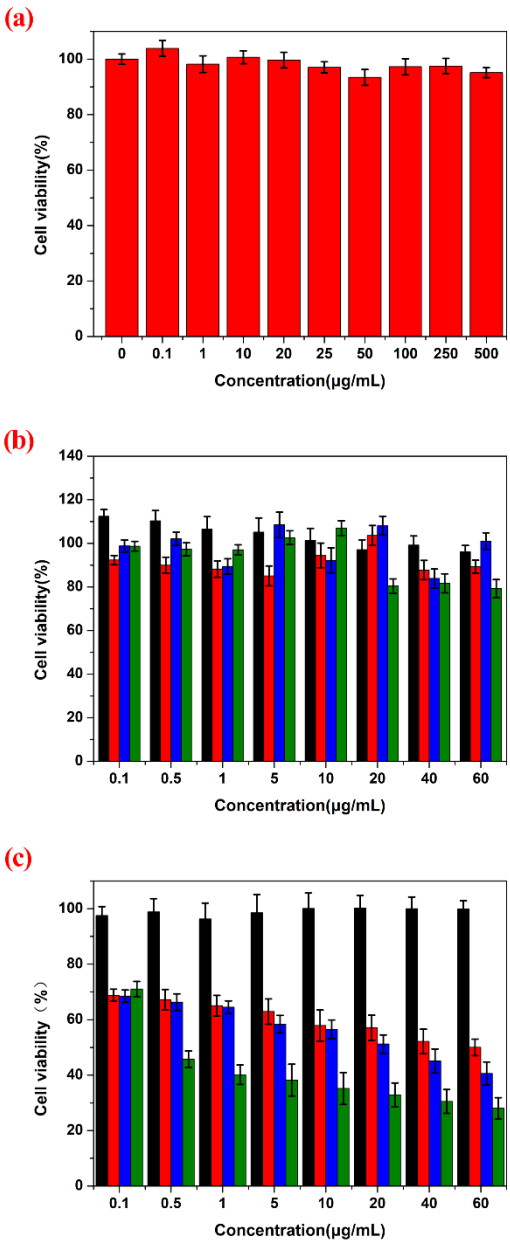

Figure 5. MTT viability results for (a) L929 cells treated with blank cross-linked micelles, (b) L929 cells and (c) H22 cells treated with PBS (black), free bufalin (red), bufalin loaded non-cross-linked micelles (blue) and bufalin loaded cross-linked micelles (green).

3.5. Confocal microscopy

Confocal laser scanning microscopy (CLSM) analysis was used to evaluate the cellular uptake of

FITC-bufalin loaded micelles into L929 cells and H22 cells (Figure 6). Strong FITC fluorescence appeared in the H22 cells after 2 h incubation with the micelles (whether cross-linked or not), demonstrating uptake. The cross-linked micelles led to the highest FITC contrast, showing that these micelles are the most effective formulation for delivering FITC-bufalin to H22 cells. In contrast, only low FITC fluorescence was seen for L929 cells after 2 h incubation with either FITC-bufalin or the drug loaded micelles. This shows that the micelles have the ability to selectively target tumor cells. The results of the CLSM experiments hence agree with the cell viabilities obtained from MTT assays.

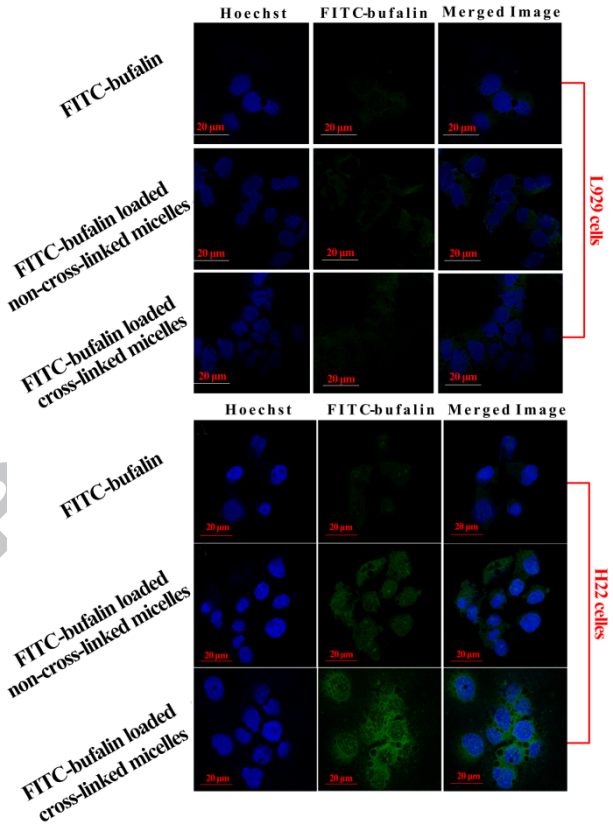

Figure 6. CLSM images of L929 or H22 cellular uptake of FITC-bufalin from the different formulations.

3.6. In vivo antitumor effects

The therapeutic performance of bufalin-loaded cross-linked micelles was investigated using H22 tumor bearing ICR mice. The mice were injected with 2 mg bufalin equiv./kg on days 0, 2, 4, 6, 8, 10,

12 and 14. Tumor growth was noticeably suppressed by the bufalin-loaded cross-linked micelles compared to mice receiving PBS injections or free bufalin (Figure 7(a)). Continuous tumor progression was witnessed for mice treated with the bufalin-loaded non-cross-linked micelles, which may be ascribed to premature release of bufalin from the unstable HOOC-F127-COOH micelles during circulation in the blood. At day 14, one representative mouse of each group was sacrificed, and the tumors collected and weighed. The size and weight of the tumors from mice treated with drug-loaded cross-linked micelles are much smaller than those isolated from the other groups (Figure 7(b)).

When the mice were treated with PBS, a continuous increase in body weight was noted (Figure 7(c)) as a result of the increasing tumor size. The mice treated with free bufalin or the micelles showed no such increase, with no noticeable change in body weight. This indicates that both the drug and micelles had low systemic toxicity. The bufalin-loaded cross-linked micelles also had profound effects in increasing the survival rates of H22-tumor bearing ICR mice (Figure 7(d)). While PBS-treated mice had survival times of just 17 days, a bufalin treatment increased this to 24 days. The non-cross-linked micelles extended the survival time (to 32 days), and the cross-linked micelles raised it further to beyond 36 days.

After sacrifice, the tumors and major organs were resected for analysis. TUNEL assay results showed no green coloration in the tumors of mice treated with PBS (Figure 8), indicating all the cells to be viable. Some green-colored cells are noticeable with all the bufalin treatments, indicative of apoptosis. The highest levels of apoptosis were seen in the tumors resected from mice treated with bufalin-loaded cross-linked micelles (Figure 8), as is clear from the increased number of green-colored cells. Therefore, the cross-linked micelles induce apoptosis more effectively than either free bufalin or the non-cross-linked system. This finding is consistent with the other *in vivo* results.

Off-target toxicity is always a concern with cancer therapies. Histological analyses of major organs post-sacrifice were thus conducted (Figure S3). The images obtained from mice treated with PBS and the drug-loaded cross-linked micelles are very similar, and hence it is clear that the micelles do not appear to have any systemic toxicity.

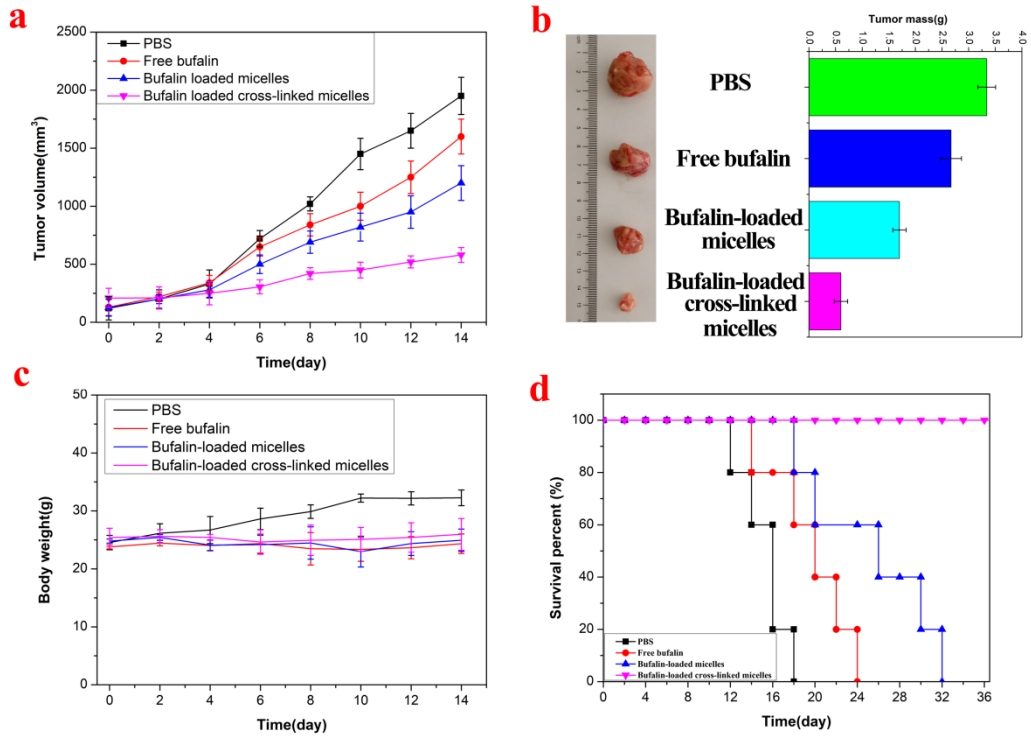

Figure 7. *In vivo* antitumor activity of different bufalin formulations in H22-tumor bearing mice. (a) Tumor volume changes with time. (b) Photographs of typical tumors isolated on day 14. (c) Body weight changes over 14 days. (d) Survival curves.

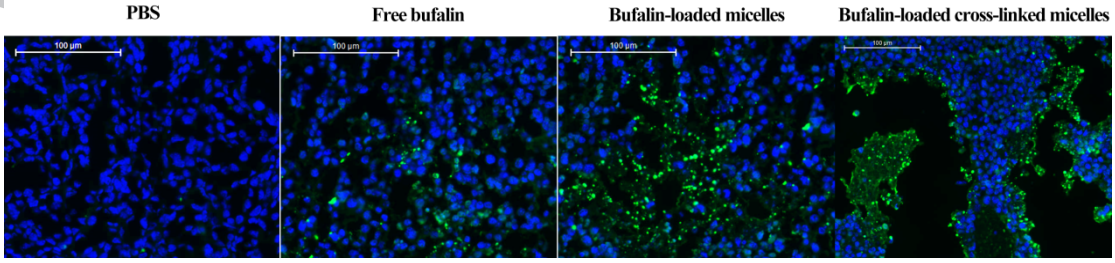

Figure 8. Representative TUNEL-stained tumor slices from the different treatment groups. Scale bars: 100 μm.

Compared to other F127-based nanoscale delivery systems reported in the literature, the thermo- and redox-responsive drug delivery system developed in this work has a number of advantages. For example, Zhang *et al.* developed doxorubicin (DOX)-loaded pheophorbide A-modified Pluronic F127 (F127) micelles for combined chemo-photodynamic therapy of melanoma (Zhang et al., 2018). While drug release was enhanced at acidic pH compared to pH 7.4 (*ca.* 60% *vs* 45% after 48 h), this pH-responsiveness was limited and the cumulative DOX release after 48 h was still low. Here, by utilizing thermo-responsive Pluronic F127-based polymer micelles to encapsulate bufalin at low temperature, a high loading capacity was achieved. Additionally, the use of cystamine as a redox-responsive cross-linker gives redox-responsive bufalin release from the micelles specifically at the target tumor site. This results in improved chemotherapeutic efficacy, as well as reduced systemic toxicity.

4. Conclusions

A thermo- and redox-responsive drug delivery system was prepared in this work, based on Pluronic F127. HOOC-F127-COOH was first prepared by functionalizing Pluronic F127 with carboxylate groups. This carboxylated Pluronic F127 ABA tri-block coplolymer was subsequently assembled into micelles. At 4 ºC, these micelles are porous and can easily take up drug from solution. When they are heated to 37 ºC they contract, holding the drug in place in their cores. By crosslinking the micelles, they can retain their drug loading regardless of temperature. A cystamine-based cross-linker was used to impart the micelles with the ability to respond to GSH in the cancer microenvironment. Before cross-linking, the micelles are ~ 281 nm in size at 4 ºC and ~ 20 nm at 37 ºC. This sensitivity was exploited to effectively incorporate the anti-cancer drug bufalin, with an encapsulation efficiency of 79.6 ± 1.2 % and a loading content of 2.9 ± 0.2 % obtained. The cross-linked F127-based micelles were highly biocompatible with healthy cells, and were more effective than free bufalin or non-cross-linked

micelles at inducing the death of cancer cells. Confocal microscopy demonstrated that the cross-linked micelles led to effective take-up of bufalin into H22 cancer cells, but uptake into healthy L929 cells was minimal. *In vivo* antitumor studies revealed that tumor growth was significantly suppressed by the bufalin-loaded cross-linked micelles, with no evident side effects. The F127-based micelles prepared in this work are thus attractive temperature and redox-responsive nanoscale delivery systems that might be applied for the targeted delivery of hydrophobic anticancer drugs to the tumor microenvironment.

Acknowledgements

This investigation was supported by grant 16410723700 from the Science and Technology Commission of Shanghai Municipality, the Biomedical Textile Materials "111 Project" of the Ministry of Education of China (No. B07024), and the UK-China Joint Laboratory for Therapeutic Textiles (based at Donghua University).

References

Arranja, A., Schroder, A.P., Schmutz, M., Waton, G., Schosseler, F., Mendes, E., 2014. Cytotoxicity

454 and internalization of Pluronic micelles stabilized by core cross-linking. J Control Release 196,
455 87-95.
456 Astafieva, I., Xing, F.Z., Eisenberg, A., 1993. Critical micellization phenomena in block
457 polyelectrolyte solutions - Macromolecules (ACS Publications). Macromolecules 26, 7339-7352.
458 Bode, S.A., Hansen, M.B., Oerlemans, R.A., van Hest, J.C., Lowik, D.W., 2015. Enzyme-Activatable
459 Cell-Penetrating Peptides through a Minimal Side Chain Modification. Bioconjug Chem 26, 850-
460 856.
461 Bohorquez, M., Koch, C., Trygstad, T., Pandit, N., 1999a. A study of the temperature-dependent
462 micellization of pluronic F127. J. Colloid Interface Sci 216, 34-40.
463 Bohorquez, M., Koch, C., Trygstad, T., Pandit, N., 1999b. A Study of the Temperature-Dependent
464 Micellization of Pluronic F127. J. Colloid Interface Sci 216, 34.
465 Cabral, H., Matsumoto, Y., Mizuno, K., Chen, Q., Murakami, M., Kimura, M., Terada, Y., Kano,
466 M.R., Miyazono, K., Uesaka, M., 2011. Accumulation of sub-100 nm polymeric micelles in
467 poorly permeable tumours depends on size. Nat Nanotech 6, 815-823.
468 Chen, D.-y., Zhang, R., Liu, Y., Zhou, T., Li, X., Gao, S., Zhang, J., Cui, X.-n., 2016. Effects of
469 cinobufacini injection on hepatocarcinoma cell proliferation, invasion and metastasis. RSC
470 Advances 6, 82417-82424.
471 Chien, Y.H., Chou, Y.L., Wang, S.W., Hung, S.T., Liau, M.C., Chao, Y.J., Su, C.H., Yeh, C.S., 2013.
472 Near-Infrared Light Photocontrolled Targeting, Bioimaging, and Chemotherapy with Caged
473 Upconversion Nanoparticles in Vitro and in Vivo. Acs Nano 7, 8516-8528.
474 Cui, L., Zhang, F., Wang, Q., Lin, H., Yang, C., Zhang, T., Tong, R., An, N., Qu, F., 2015. NIR light
475 responsive core–shell nanocontainers for drug delivery. J. Mater. Chem. B 3, 7046-7054.

476 Ding, H., Yong, K.T., Law, W.C., Roy, I., Hu, R., Wu, F., Zhao, W., Huang, K., Erogbogbo, F.,
477 Bergey, E.J., Prasad, P.N., 2011. Non-invasive tumor detection in small animals using novel
478 functional Pluronic nanomicelles conjugated with anti-mesothelin antibody. Nanoscale 3, 1813-
479 1822.
480 Duan, X., Xiao, J., Yin, Q., Zhang, Z., Yu, H., Mao, S., Li, Y., 2013. Smart pH-Sensitive and
481 Temporal-Controlled Polymeric Micelles for Effective Combination Therapy of Doxorubicin and
482 Disulfiram. Acs Nano 7, 5858-5869.
483 Ekaterina B. Zhulina, Chandralekha Singh, ‡ and, Anna C. Balazs, 1996. Self-Assembly of Tethered
484 Diblocks in Selective Solvents. Macromolecules 29, 8254-8259.
485 Estrela, J.M., Ortega, A., Obrador, E., 2006. Glutathione in cancer biology and therapy. Crit Rev Cl
486 Lab Sci 43, 143-181.
487 Fan, W., Liu, L., Zhao, H., 2017. Co-assembly of Patchy Polymeric Micelles and Protein Molecules.
488 Angew Chem Int Ed 56, 8844-8848.
489 Fang, Y., Jiang, Y., Zou, Y., Meng, F., Zhang, J., Deng, C., Sun, H., Zhong, Z., 2017. Targeted glioma
490 chemotherapy by cyclic RGD peptide-functionalized reversibly core-crosslinked multifunctional
491 poly(ethylene glycol)-b-poly(epsilon-caprolactone) micelles. Acta Biomater 50, 396-406.
492 Fischer, D., Li, Y., Ahlemeyer, B., Krieglstein, J., Kissel, T., 2003. In vitro cytotoxicity testing of
493 polycations: influence of polymer structure on cell viability and hemolysis. Biomaterials 24, 1121.
494 Gothwal, A., Khan, I., Gupta, U., 2016. Polymeric Micelles: Recent Advancements in the Delivery of
495 Anticancer Drugs. Pharm Res 33, 18-39.
496 Han, Y., Jing, J., Jie, C., Wei, J., 2016. Effect of hydrophilicity of end-grafted polymers on protein
497 adsorption behavior: A Monte Carlo study. Colloids Surf. B: Biointerfaces 142, 38-45.

Hu, Q., Liang, B., Sun, Y., Guo, X.L., Bao, Y.J., Xie, D.H., Zhou, M., Duan, Y.R., Yin, P.H., Peng, Z.H., 2014. Preparation of bufalin-loaded pluronic polyetherimide nanoparticles, cellular uptake, distribution, and effect on colorectal cancer. Int J Nanomedicine 9, 4035-4041.

Jensen, A.I., Severin, G.W., Hansen, A.E., Fliedner, F.P., Eliasen, R., Parhamifar, L., Kjaer, A., Andresen, T.L., Henriksen, J.R., 2018. Remote-loading of liposomes with manganese-52 and in vivo evaluation of the stabilities of (52)Mn-DOTA and (64)Cu-DOTA using radiolabelled liposomes and PET imaging. J Control Release 269, 100-109.

Jin, Q., Li, H., Jin, Z., Huang, L., Wang, F., Zhou, Y., Liu, Y., Jiang, C., Oswald, J., Wu, J., Song, X., 2018. TPGS modified nanoliposomes as an effective ocular delivery system to treat glaucoma. Int J Pharm 553, 21-28.

Li, N., Wang, J., Yang, X., Li, L., 2011. Novel nanogels as drug delivery systems for poorly soluble anticancer drugs. Colloids Surf. B: Biointerfaces 83, 237-244.

Li, Y., Maciel, D., Rodrigues, J.o., Shi, X., Tomás, H., 2015. Biodegradable polymer nanogels for drug/nucleic acid delivery. Chem Rev 115, 8564-8608.

Liang, H., Ren, X., Qian, J., Zhang, X., Meng, L., Wang, X., Li, L., Fang, X., Sha, X., 2016. Size-Shifting Micelle Nanoclusters Based on a Cross-Linked and pH-Sensitive Framework for Enhanced Tumor Targeting and Deep Penetration Features. ACS Appl Mater Interfaces 8, 10136-10146.

Lin, L.S., Yang, X., Niu, G., Song, J., Yang, H.H., Chen, X., 2016. Dual-enhanced photothermal conversion properties of reduced graphene oxide-coated gold superparticles for light-triggered acoustic and thermal theranostics. Nanoscale 8, 2116-2122.

Liu, J., Zhang, B., Luo, Z., Ding, X., Li, J., Dai, L., Zhou, J., Zhao, X., Ye, J., Cai, K., 2015. Enzyme

responsive mesoporous silica nanoparticles for targeted tumor therapy in vitro and in vivo. Nanoscale 7, 3614-3626.

Meng, Z., Yang, P., Shen, Y., Bei, W., Zhang, Y., Ge, Y., Newman, R.A., Cohen, L., Liu, L., Thornton, B., Chang, D.Z., Liao, Z., Kurzrock, R., 2009. Pilot study of huachansu in patients with hepatocellular carcinoma, nonsmall-cell lung cancer, or pancreatic cancer. Cancer 115, 5309-5318.

Newman, R.A., Yang, P., Pawlus, A.D., Block, K.I., 2008. Cardiac glycosides as novel cancer therapeutic agents. Mol Interv 8, 36.

Northfelt, D.W., Martin, F.J., Working, P., Volberding, P.A., Russell, J., Newman, M., Amantea, M.A., Kaplan, L.D., 2013. Doxorubicin encapsulated in liposomes containing surface-bound polyethylene glycol: pharmacokinetics, tumor localization, and safety in patients with AIDS-related Kaposi's sarcoma. J Clin Pharmacol 36, 55-63.

Rao, W., Wang, H., Han, J., Zhao, S., Dumbleton, J., Agarwal, P., Zhang, W., Zhao, G., Yu, J., Zynger, D.L., 2015. Chitosan-Decorated Doxorubicin-Encapsulated Nanoparticle Targets and Eliminates Tumor Reinitiating Cancer Stem-like Cells. Acs Nano 9, 5725-5740.

Roointan, A., Farzanfar, J., Mohammadi-Samani, S., Behzad-Behbahani, A., Farjadian, F., 2018. Smart pH responsive drug delivery system based on poly(HEMA-co-DMAEMA) nanohydrogel. Int J Pharm 552, 301-311.

Sutton, D., Nasongkla, N., Blanco, E., Gao, J., 2007. Functionalized micellar systems for cancer targeted drug delivery. Pharm Res 24, 1029-1046.

Takai, N., Ueda, T., Nishida, M., Nasu, K., Narahara, H., 2008. Bufalin induces growth inhibition, cell cycle arrest and apoptosis in human endometrial and ovarian cancer cells. Int J Mol Med 21, 637-

643.

Tseng, W.C., Jong, C.M., 2003. Improved stability of polycationic vector by dextran-grafted branched polyethylenimine. Biomacromolecules 4, 1277-1284.

Wang, H., Zhao, Y., Wu, Y., Hu, Y.L., Nan, K., Nie, G., Chen, H., 2011. Enhanced anti-tumor efficacy by co-delivery of doxorubicin and paclitaxel with amphiphilic methoxy PEG-PLGA copolymer nanoparticles. Biomaterials 32, 8281-8290.

Wang, Y., Lonard, D.M., Yu, Y., Chow, D.C., Palzkill, T.G., Wang, J., Qi, R., Matzuk, A.J., Song, X., Madoux, F., Hodder, P., Chase, P., Griffin, P.R., Zhou, S., Liao, L., Xu, J., O'Malley, B.W., 2014. Bufalin is a potent small-molecule inhibitor of the steroid receptor coactivators SRC-3 and SRC-1. Cancer Res 74, 1506-1517.

Wu, J., Williams, G.R., Branford-White, C., Li, H., Li, Y., Zhu, L.-M., 2016. Liraglutide-loaded poly (lactic-co-glycolic acid) microspheres: Preparation and in vivo evaluation. Eur J Pharm Sci 92, 28-38.

Xu, Z., Liu, S., Kang, Y., Wang, M., 2015. Glutathione-Responsive Polymeric Micelles Formed by a Biodegradable Amphiphilic Triblock Copolymer for Anticancer Drug Delivery and Controlled Release. ACS Biomate Sci Eng 1, 585-592.

Yang, K., Feng, L., Shi, X., Liu, Z., 2013. Nano-graphene in biomedicine: theranostic applications. Chem Soc Rev 42, 530-547.

Yanzuo, C., Wei, Z., Yukun, H., Feng, G., Xianyi, S., Xiaoling, F., 2015. Pluronic-based functional polymeric mixed micelles for co-delivery of doxorubicin and paclitaxel to multidrug resistant tumor. Int J Pharm 488, 44-58.

Yu, C.H., Kan, S.F., Pu, H.F., Jea Chien, E., Wang, P.S., 2008. Apoptotic signaling in bufalin- and

564 cinobufagin-treated androgen-dependent and -independent human prostate cancer cells. Cancer
565 Sci 99, 2467-2476.
566 Zhang, C., Zhang, J., Qin, Y., Song, H., Huang, P., Wang, W., Wang, C., Li, C., Wang, Y., Kong, D.,
567 2018. Co-delivery of doxorubicin and pheophorbide A by pluronic F127 micelles for chemo-
568 photodynamic combination therapy of melanoma. J. Mater. Chem. B.
569 2018:10.1039.C7TB03179C.
570 Zhang, W., Gilstrap, K., Wu, L., Rb, K.C., Moss, M.A., Wang, Q., Lu, X., He, X., 2010. Synthesis and
571 characterization of thermally responsive Pluronic F127-chitosan nanocapsules for controlled
572 release and intracellular delivery of small molecules. Acs Nano 4, 6747-6759.
573 Zhang, Y., Song, W., Geng, J., Chitgupi, U., Unsal, H., Federizon, J., Rzayev, J., Sukumaran, D.K.,
574 Alexandridis, P., Lovell, J.F., 2016. Therapeutic surfactant-stripped frozen micelles. Nat Commun
575 7, 11649.
576 Zhao, X., Liu, P., 2015. Reduction-responsive core-shell-corona micelles based on triblock
577 copolymers: novel synthetic strategy, characterization, and application as a tumor
578 microenvironment-responsive drug delivery system. ACS Appl Mater Interfaces 7, 166-174.
579 Zhu, Y., Wang, X., Zhang, J., Meng, F., Deng, C., Cheng, R., Feijen, J., Zhong, Z., 2017. Exogenous
580 vitamin C boosts the antitumor efficacy of paclitaxel containing reduction-sensitive shell-
581 sheddable micelles in vivo. J Control Release 250, 9-19.
582 Zou, Y., Fang, Y., Meng, H., Meng, F., Deng, C., Zhang, J., Zhong, Z., 2016. Self-crosslinkable and
583 intracellularly decrosslinkable biodegradable micellar nanoparticles: A robust, simple and
584 multifunctional nanoplatform for high-efficiency targeted cancer chemotherapy. J Control Release
585 244, 326-335.

586

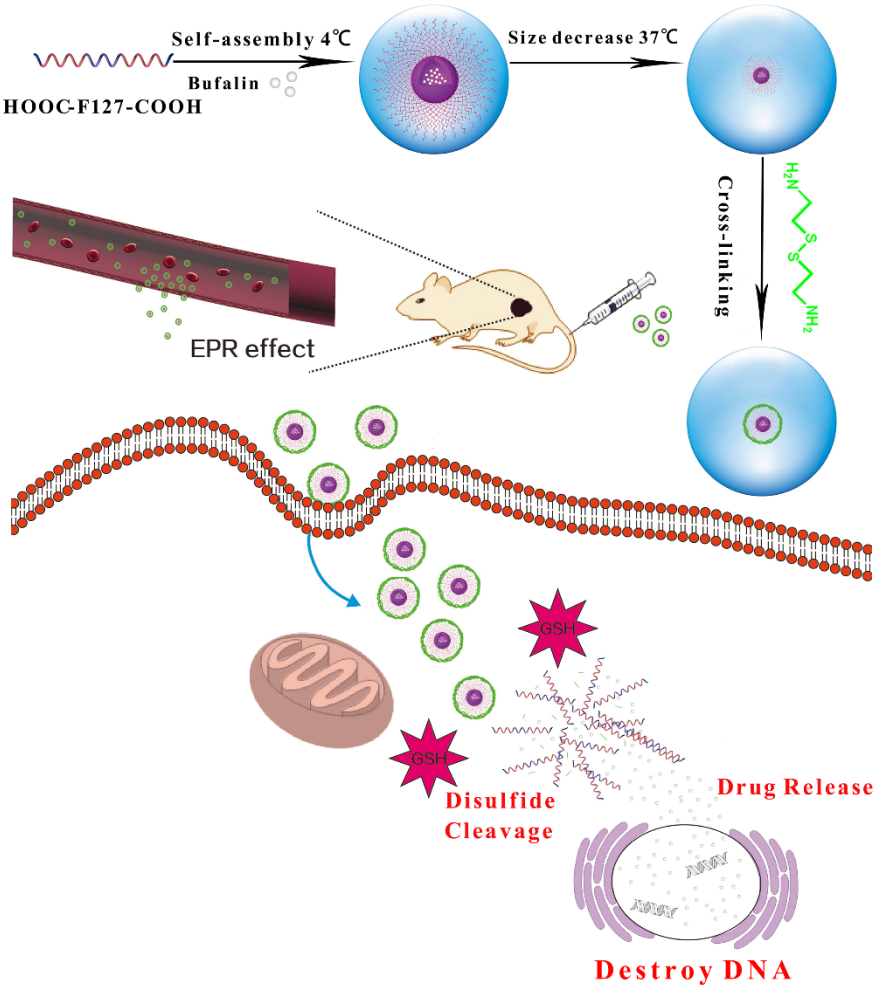

587

588